ISSN: 2230-9926

Available online at http://www.journalijdr.com

IJDR

International Journal of Development Research
Vol. 08, Issue, 05, pp.20253-20259, May, 2018

ORIGINAL RESEARCH ARTICLE OPEN ACCESS

SIZING OF A REVOLVING CRANE FOR CARGO HANDLING UP TO 5000 N

[1,*]Vilson Menegon Bristot, [1]Leopoldo Pedro Guimarães Filho, [1]Kristian Madeira, [2]Vilmar MenegonBristot and [3]Márcio José Meisen Júnior

[1]UNESC, Universidade do Extremo Sul Catarinense – NEEP – Núcleo de Estudos em Engenharia de Produção - Santa Catarina, Brasil
[2]Vilmar MenegonBristot - IFSC, Instituto Federal de Santa Catarina - Santa Catarina, Brasil
[3]Márcio José Meisen Júnior - SATC, Faculdade - Santa Catarina, Brasil

ARTICLE INFO

Article History:
Received 18th February, 2018
Received in revised form
10th March, 2018
Accepted 27th April, 2018
Published online 28th May, 2018

Key Words:
Project; slewing crane;
Road equipment.

ABSTRACT

This study aimed to design a revolving crane, to be deployed in the cutting industry and folds into a manufacturer of road equipment. The implementation of the project aims to increase productivity, significantly reducing the existing idle capacity in this sector, due to waiting for the use of the crane, when there is the need for handling heavy parts. For the development of crane design, all significant requests, scaling all the structural part and the elements necessary for the construction machines were used. After sizing of all design elements, it was used Ansys® software, which also allowed a comparison of the results obtained. Recitations of the whole rotating crane components were performed in Solid Edge® design software and the material chosen for crane structure was steel ASTM A36 for its machinability, weldability and mechanical strength, and for being one of the most widely used steel for structures metal.

Citation: Vilson Menegon Bristot, Leopoldo Pedro Guimarães Filho, Kristian Madeira, Vilmar MenegonBristot and Márcio José Meisen Júnior, 2018. "Sizing of a revolving crane for cargo handling up to 5000 N", *International Journal of Development Research*, 8, (05), 20253-20259.

INTRODUCTION

The highways are the most widely used means of transport for cargo handling in Brazil, generating a growing demand for road equipment. The sector companies seeking continuous improvements in its manufacturing processes in order to reduce costs, increase productivity and quality of their products, thus ensuring greater market competitiveness and customer satisfaction. In the studied road equipment company, production is divided into several sectors. The cutting and bending sector is where it begins the process of manufacturing parts for assembly, and has the following machines installed: two guillotines, two folding machines, four mechanical presses and a crane. Through cronoanalíticos data, it was found that the bottleneck of the process the rated sector is in the drive parts with the bridge crane, since all machines rely on a single crane to setup exchange parts, there being idleness in the process, generated by the expected use this crane to move heavy parts, as shown in Fig. 1.

Corresponding author: **Vilson Menegon Bristot,**
UNESC, Universidade do Extremo Sul Catarinense – NEEP – Núcleo de Estudos em Engenharia de Produção - Santa Catarina, Brasil.

Thus, the present study aims to design a revolving crane to be deployed in the cutting and bending sector, to increase productivity, facilitate the handlings of parts and reduce and / or eliminate idle between processes.

Literature Review

A complete probabilistic procedure was performed to assess the damage by fatigue cranes. The study showed that for every type of crane is required a thorough analysis of the workplace, length of service and different loads, and thus cannot draw up a generic procedure (Bucas *et al*., 2014). It is estimated that when designing the load structure of a crane, a static analysis is still important for the preliminary determination of the required dimensions. However, to bring the results of these calculations closest to reality, different static procedures are introduced. These procedures take into account various dynamic effects by appropriate coefficients. In this work, a new process is proposed for the determination of the maximum horizontal inertia forces in a radial direction that are acting on a suspended load arm during the rotational movement of a crane.

(a) (b) (c)

Fig. 1. Cutting sector and bending: a - machine setup with the crane, b - bending heavy parts with the help of the crane, c - cutting guillotine heavy plates with the help of the crane

Based on this, a new coefficient radial horizontal inertia force is introduced, and is a diagram calculated for the rapid determination of this coefficient (Jerman and Kramar, 2008). A method was performed to control the turning motion of mobile cranes. The method allows the transportation of cargo to a chosen point and ensures the minimization of its oscillations when the move is complete. The model of the drive system is controlled hydraulically. The research confirms the use of the hydraulic system for controlling the turning motion of the crane (Kłosiński, 2005). It conducted a logical model for the quantification of occupational risks in the event of collapse or falling cranes. The logical interdependencies of the various events involved with the fall of an object or crane and its consequences in the study are simulated. This logic model consists of two main parts: the part incorporating the events that preceded the falling object and the part incorporating events after the fall of the object in a person. Three severity levels are considered; lethal injuries; non-lethal injuries permanent and retrievable injuries (Aneziris *et al*., 2008). A study on the anti-sway control and tracking for mobile cranes was executed. The aim of this control is free shipping crane load balancing, making account commands crane operator. Based on the mathematical model and linearization, sought to stabilize the control laws for turning and movement, using the linearization approach input / output. Operator controls are smoothed in line for a trajectory generator responded by entry restrictions (Neupert *et al*., 2010). A study was conducted over the life of a bearing based on the revolutions (or time period). The operating load and speed are the main factors to estimate the life of the bearing. In this study, he noted that the premature failure was attributed to misalignment of the bearing, which led to the uneven distribution of load rollers and raceway (Ghosh and Gurumoorthy, 2013). It conducted a study of catastrophic failure of cranes. The two cranes failures are discussed in this study. Both spears have different designs, but the common causes have been identified, related to deficiencies in the design and construction of its bases. Striking similarities in fault conditions are discussed in this study. These include errors in the identification and interpretation of previous symptoms, the mitigation measures and risks taken by staff, due to lack of information and training (Marquez *et al*., 2014).

MATERIALS AND METHODS

To begin the study, first, was collecting information on the maximum load that the crane should support as necessary moves to ensure a better work performance. According to the arrangement of machines in the industry, there is a need of boom reach dimensions that are 5 m in length with a height of 3.5 m and a rotary movement of 270 °. To establish the best position of the crane in the doubles court, it was used design software Auto CAD®. Recitations of the components of the whole rotating crane in design software Solid Edge® were performed. For the design of the rotary crane, the maximum load of 5000 N was set, and added 300 N to compensate for the weight of the chain hoist. We adopted a compensation coefficient $\Psi = 1.9$ (Dubbel, 1974), thereby defining a load "P" = 10070 N. When dimensioning was also considered the own weight of all the elements of the metal structure. The data of the materials used to perform the calculations are shown in Tab. 1. (Açominas, 2003)

Table 1. Data of the materials used

Material	Coarseness m [N/m]	Moment of inertia I [m^4]	Section area S [m²]
Profile "W"	284	4046E-8	36,6E-4
Flat bar	76	20,81E-8	9,67E-4
Square bar	809,6	887,96E-8	103,22E-4
Tube of 14"	1947	34338,79E-8	248,28E-4

Structural Steel

The steel chosen for the project was the A36, whose properties are specified by ASTM A36. For (Favorit, 2012), it is a good weldability steel, medium strength and machinability medium. According to [http://www.lume.ufrgs.br/bitstream/handle/10183/6662/000488009.pdf?sequence=1&locale=en], ASTM A36 Standard determines the range corresponding to the tensile strength 400-550 MPa and the yield strength of 250 MPa. These data are confirmed by (Hibbeler, 2005) which also indicate that the modulus of elasticity of the material is 200 GPa. For this study, the endurance limit was set at 240 MPa and the yield strength of the shear was set at 120 MPa.

Metal Structure

We analyzed all the efforts that the metal structure can be submitted during the work, with the position of the boom to 135 °. To validate the results, the deformations were calculated and equivalent strains using classical mechanics and the fundamentals of strength of materials, and also the Ansys®

software, allowing comparison of results, proving the calculations.

Profile "W"

The profile "W" gauge 250 x 28.9 mm with a length of 5 m, is the boom of the crane, and works as rail for moving the chain hoist, manually over its entire length with the help of bearings. In Fig. 2, contains the cross section and the free-body diagram. The supports were the points "C" and "D". Two load situations have been conducted, making the analysis of the most critical points of maximum deflection: The first analysis was applied load at point "A" and the second analysis with the load at point "B", and to calculate the remaining the structure of the slewing crane load was considered only at point "B". To determine the best location of the point "D" support the boom, it was found that the angles of inclination to the two situations charges should be the same at point "D", thus making a better displacement of the chain hoist.

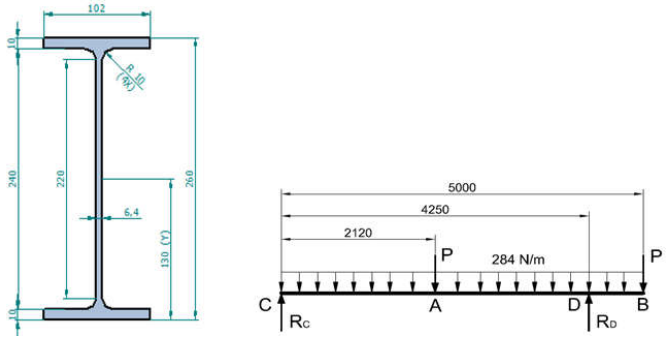

Fig. 2. Profile "W" gauge 250 X 28.9 mm. a - cross section, b- free body diagram

To calculate the maximum deflection the points "A" and "B" and the tilt angle at point "D", first, it was necessary to perform the calculation of the sum of the moments with respect to point "C". There was thus obtained the vertical reaction at the point "D", can be described by Eq. (1) where the value of "X" was replaced by the distance of the applied loads. For the first analysis where the load was applied at point "A", the value of "X" has been replaced by the distance of 2.12 m. For the second analysis where the load is applied at point "B", a value "X" was replaced by the distance of 5.0 m.

$$\sum M_C = 0 \ \therefore \ R_D = \frac{3550+10070 \cdot X}{4{,}25} \text{[N]} \ \ldots\ldots\ldots\ldots\ldots\ldots\ldots\ldots\ldots\ldots (1)$$

Then, the sums of the vertical forces were used to find the reaction in the "C" dot may be described by Eq. (2):

$$\sum F_y = 0 \ \therefore \ R_C = 284 \cdot 5 + 10070 - R_D \quad \text{[N]} \ \ldots\ldots\ldots\ldots\ldots (2)$$

To obtain the equation governing the behavior of the elastic line at point "A" and at point "B", Eq. (3) (Beer et al., 1995) was used:

$$\frac{d^2y}{dx^2} = \frac{M(x)}{E \cdot I} \quad [\text{m}^{-1}] \ \ldots\ldots\ldots\ldots\ldots\ldots\ldots\ldots\ldots\ldots\ldots\ldots\ldots\ldots\ldots\ldots (3)$$

By analyzing the load at point "A", the equation of the bending moment M (x) can be described by Eq. (4), according to classical mechanics:

$$M(x) = R_C \cdot X - \frac{284 \cdot X^2}{2} - 10070 \cdot \langle X - 2{,}12 \rangle + R_D \cdot \langle X - 4{,}25 \rangle \text{[N.m]} \quad \ldots\ldots\ldots\ldots (4)$$

Similarly for the load at point "B", the equation of the bending moment M (x) can be described by Eq. (5):

$$M(x) = R_C \cdot X - \frac{284 \cdot X^2}{2} + R_D \cdot \langle X - 4{,}25 \rangle \text{[N.m]} \quad \ldots\ldots\ldots\ldots\ldots\ldots (5)$$

The slope or slope angle was calculated from the equation of curvature, described by Eq. (6) (Beer *et al*., 1995):

$$\frac{dy}{dx} = \int_0^x \frac{M(x)}{E \cdot I} \quad \text{[rad]} \ \ldots\ldots\ldots\ldots\ldots\ldots\ldots\ldots\ldots\ldots\ldots\ldots\ldots\ldots\ldots\ldots (6)$$

The maximum or maximum displacement was calculated by integrating the equation of curvature twice, and can be described by Eq. (7) (Beer *et al*., 1995):

$$\gamma = \iint_0^x \frac{M(x)}{E \cdot I} \text{[m]} \ \ldots\ldots\ldots\ldots\ldots\ldots\ldots\ldots\ldots\ldots\ldots\ldots\ldots\ldots\ldots\ldots (7)$$

To calculate the maximum normal stress σ, the maximum moment M_ (Max) was used with the load being applied at the point "A" and the flexural modulus W_x, together with the axial force F_x in the profile, which can be described by Eq (8), Eq. (9) and Eq. (10), respectively [Beer *et al*., 1995]:

$$M_{Máx.} = R_C \cdot 2{,}12 - \frac{(284 \cdot 2{,}12^2)}{2} \quad \text{[N.m]} \ \ldots\ldots\ldots\ldots\ldots\ldots\ldots\ldots (8)$$

$$W = \frac{I}{y} \quad [\text{m}^3] \ \ldots\ldots\ldots\ldots\ldots\ldots\ldots\ldots\ldots\ldots\ldots\ldots\ldots\ldots\ldots\ldots (9)$$

$$\sigma = \pm \frac{M_{Máx.}}{W_x} \pm \frac{F_x}{S} \text{[Pa]} \ \ldots\ldots\ldots\ldots\ldots\ldots\ldots\ldots\ldots\ldots\ldots\ldots\ldots\ldots\ldots\ldots (10)$$

Flat Bar

The flat bar has been placed in the structure as a rod to increase the rigidity of the "W" profile, where one of its ends is welded to the shaft and the other is welded to the "W" profile. The cross section of the flat bar is shown in Fig. 4:

Fig. 4. Cross section and the total length of the flat bar

The flat bar undergoes only tensile force, which can be described by Eq. (11), and then the normal stress was calculated to determine the minimum area, as described by Eq. (12) [Beer *et al*., 1995]:

$$F_1 = \frac{R_D}{sen 11{,}84^\circ} \text{[N]} \ \ldots\ldots\ldots\ldots\ldots\ldots\ldots\ldots\ldots\ldots\ldots\ldots\ldots\ldots\ldots\ldots (11)$$

$$A_b = \frac{F_1}{\sigma_a} [\text{m}^2] \ \ldots\ldots\ldots\ldots\ldots\ldots\ldots\ldots\ldots\ldots\ldots\ldots\ldots\ldots\ldots\ldots (12)$$

The deformation in the length of the bar was calculated to check the displacement of the "B" point of the "W" profile, represented by Eq. (13):

$$\delta = \frac{F_1 \cdot L}{S \cdot E}\,[\mathrm{m}] \quad (13)$$

Spinning Axis

The pivot shaft was used to rotate the "W" profile, allowing a 270 ° displacement, with the help of two bearings. A four-inch square bar was used to obtain a better fit of the "W" profile and flat bar. The square bar was machined at the ends to allow for the fitting of the bearings. To perform the analysis of the axis, two free-body diagrams were devised: in the first diagram the minimum shaft diameter was obtained, considering the force at the beginning of the machined recess. In the second diagram, the maximum arrow was checked, considering the bearing in the center of the bearing. The dimensions of the axis of rotation and its free-body diagrams are shown in Fig. 5:

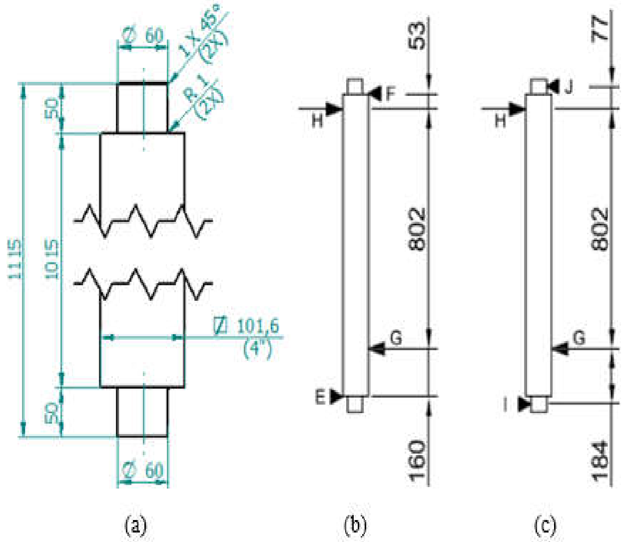

Fig. 5. Turning axis: a - side view, b - free body diagram to check the minimum diameter, c - free body diagram to check the maximum arrow

The "W" profile was fixed at the "G" point of the shaft, and the flat bar was fixed at the "H" point. The force at the point "G" has the same value of the horizontal force at the "H" point, since they are binary forces. To calculate the force at the point "G" and "H", the sum of the moments with respect to the "G" point was applied, considering the load and the weight of its metallic structure, verified in Eq. (14):

$$\sum M_G = 0 \;\therefore\; F_H = \frac{76\cdot 4{,}33\cdot 4{,}25}{2\cdot 0{,}8} + \frac{284\cdot 5^2}{2\cdot 0{,}8} + \frac{10070\cdot 5}{0{,}8}\,[\mathrm{N}] \quad (14)$$

In order to calculate the minimum diameter of the axis of rotation, it was first necessary to calculate the sum of the moments in relation to the point "F", in order to find the force at the point "E", being the same force for the point "F" Can be described by Eq. (15):

$$\sum M_F = 0 \;\therefore\; F_E = \frac{F_G\cdot 0{,}855 - F_H\cdot 0{,}053}{1{,}015}\,[\mathrm{N}] \quad (15)$$

After obtaining the necessary radial forces to calculate the minimum diameter of the axis, Eq. (16) which governs the shear stress, Eq. (17) and Eq. (18), which governs the static moment to the neutral line, and the moment of inertia, to write Eq. (19), which calculates the minimum shaft diameter (Beer and Johnston, 1995).

$$\tau = \frac{V\cdot Q}{I\cdot 2\cdot r}\,[\mathrm{Pa}] \quad (16)$$

$$Q = A_t \cdot \bar{y} \quad [\mathrm{m}^3] \quad (17)$$

$$I = \frac{\pi\cdot r^4}{4}\,[\mathrm{m4}] \quad (18)$$

$$d = 2\cdot\left(\sqrt{\frac{V\cdot 4}{\tau\cdot\pi\cdot 3}}\right)[\mathrm{m}] \quad (19)$$

In order to verify the maximum axis velocity, the forces acting at the points "I" and "J" were first found, and these binary forces were verified by the sum of the moments in relation to the point "I", described by Eq. (20):

$$\sum M_I = 0 \;\therefore\; F_J = \frac{F_H\cdot 0{,}986 - F_G\cdot 0{,}184}{1{,}063}\,[\mathrm{N}] \quad (20)$$

To find the equation governing the behavior of the elastic line, Eq. (3) was used. The M (x) described by Eq. (21):

$$M(x) = -F_I\cdot X + F_G\cdot < X - 0{,}184 > -F_H\cdot < X - 0{,}986 > \;[\mathrm{N.m}] \quad (21)$$

The maximum or maximum displacement was calculated by Eq. (7). By analyzing two points of the axis, the direct influence on the vertical displacement of the "W" profile could be verified. The arrow was verified in the distance of the axis of 0,184 m and for distance of 0,986 m. The sum of the displacements was effected through Eq. (22), where the displacement at the tip of the profile "W" is verified by Eq. (23):

$$\gamma_{total} = \gamma_{(0{,}184)} + \gamma_{(0{,}986)}\,[\mathrm{m}] \quad (22)$$

$$\text{Displacement at point "B" of profile "W"} = \frac{5\cdot\gamma_{total}}{0{,}802}\,[\mathrm{m}] \quad (23)$$

Central Columns

The central column supports the entire structure of the rotating crane, and is embedded in a block of concrete that must be sized according to the type of soil. In the concrete foundation are bolted screws leaving the spare for fixing through hexagonal nuts the base plate. The base plate was welded to the bottom of the central column, where six reinforcements were used to ensure that no cracks occurred in the weld. At the top of the column, the end stops of the "W" profile were soldered, which determined the turning direction of the crane. The upper and lower axle plates were also welded, which were used as supports for the bushings. The components of the column can be checked in Fig. 6:

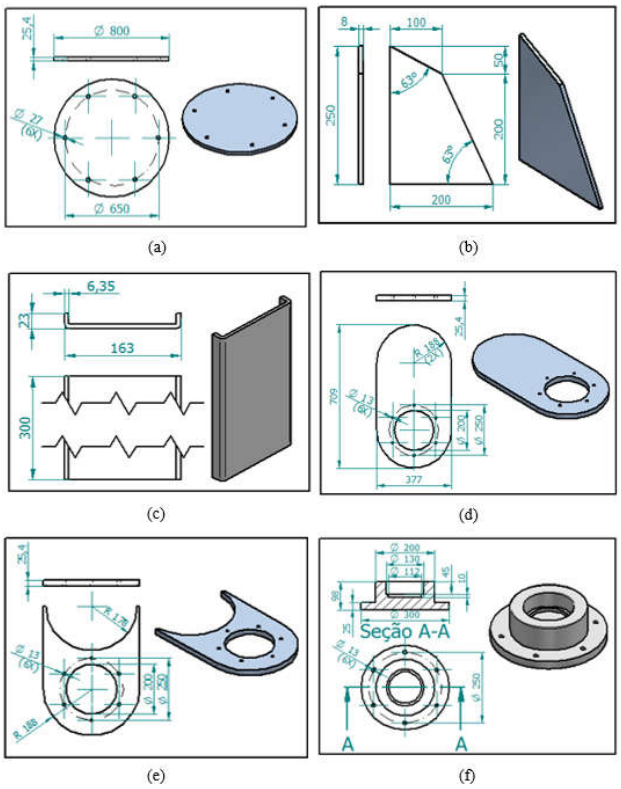

Fig. 6. Components of the central column: a - base plate, b - lower base reinforcement, c - stop, d - upper plate, e - lower plate, f - bearing bushing

The central column was designed with a round tube whose dimensions and free-body diagram can be observed as shown in Fig. 7:

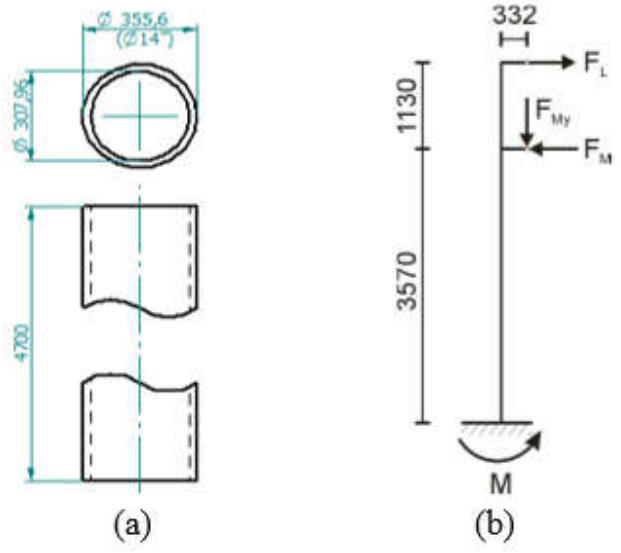

Fig. 7. Round tube: top view and front view, b- free body diagram to check the maximum arrow

In order to calculate the maximum velocity, the forces at the "L" and "M" points were first found, and these binary forces were applied by applying the sum of the moments in relation to the "L" point described by Eq. (24) :

$$\sum M_L = 0 \;\therefore\; F_M = \frac{F_I \cdot 1{,}036 - F_J \cdot 0{,}027}{1{,}13}\,[\mathrm{N}] \ldots\ldots\ldots\ldots\ldots\ldots\ldots\ldots\ldots\ldots (24)$$

To find the equation governing the behavior of the elastic line, Eq. (3) was used. The M (x) described by Eq. (25):

$$M(x) = -M + F_M \cdot \langle X - 3{,}57 \rangle \; + 0{,}332 \cdot F_{My} \cdot \langle X - 3{,}57 \rangle^0\,[\mathrm{N.m}] \ldots\ldots\ldots\ldots\ldots\ldots\ldots\ldots\ldots\ldots\ldots\ldots\ldots\ldots\ldots\ldots\ldots\ldots\ldots\ldots (25)$$

The maximum or maximum displacement was calculated by Eq. (7), where its greatest displacement was obtained in the distance of 4.7 m. To verify the displacement at point "B" of profile "W", Eq. (26) was used:

$$\textit{Displacement at the point}\ \text{"B" of the profile "W" as a function of the central columns} = \frac{5 \cdot \gamma}{4{,}7}\,[\mathrm{m}] \ldots\ldots\ldots\ldots\ldots\ldots\ldots\ldots\ldots\ldots\ldots\ldots\ldots\ldots\ldots\ldots\ldots\ldots\ldots\ldots (26)$$

By summing the maximum arrows of the rotating crane components, it was possible to check the maximum displacement at the end in profile "W" through Eq. (27):

$$\gamma_{\text{mxiumum}} = \gamma_{(Profile\ "W")} + \gamma_{(Rotating\ axis)} + \gamma_{(Central\ columns)} + \delta_{(Flat\ bar)}[\mathrm{m}] \ldots\ldots\ldots\ldots\ldots\ldots\ldots\ldots\ldots\ldots\ldots\ldots\ldots\ldots\ldots\ldots\ldots\ldots\ldots\ldots (27)$$

Scrolling and Fixing Elements

In order to realize the rotation of the axis, two bearings of a race of conical rollers were used, these being mounted against each other. To select the bearing, the minimum shaft diameter and its radial and axial loads were considered. The selected bearing was numbered 32312, according to the ISO standard, the main dimensions can be checked in Fig. 8:

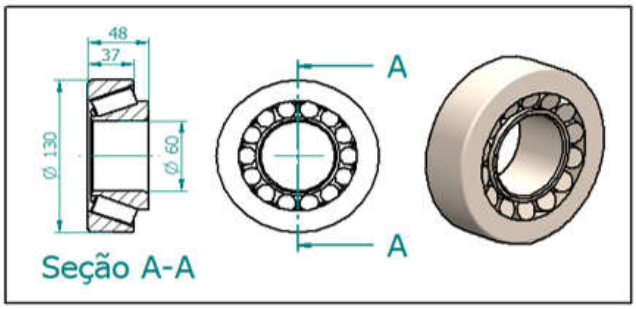

Fig. 8. View in three dimensions and view in total section

For the axial load, all the forces acting on the bearing in the vertical direction were considered, and for the radial load the force "FJ" obtained in Eq. (20) was considered. The minimum shaft diameter can be verified by Eq. (19). Its nominal life was calculated in hours, assuming a reliability of 90%, according to Eq. (28) (Melconian and Sarkis, 2000):

$$Lxh = \frac{10^6}{60 \cdot n}\left(\frac{Cr_{corrig}}{P_o}\right)^{\frac{10}{3}}\,[\mathrm{h}] \ldots\ldots\ldots\ldots\ldots\ldots\ldots\ldots\ldots\ldots\ldots\ldots\ldots\ldots\ldots\ldots\ldots\ldots\ldots\ldots (28)$$

The speed in the turning motion is very low, so for the calculation of the bearing was considered static load, being adopted a rotation of 20 rpm to stipulate the nominal life in hours of the bearing. Afterwards, the coefficient of static load was verified through Eq. (29) (Melconian and Sarkis, 2000):

$$N = \frac{Cor}{P_o} \ldots\ldots\ldots\ldots\ldots\ldots\ldots\ldots\ldots\ldots\ldots\ldots\ldots\ldots\ldots\ldots\ldots\ldots\ldots\ldots\ldots\ldots\ldots\ldots\ldots\ldots (29)$$

The bolts used in the crane were selected according to the ISO standard. In order to fasten the bushings to the upper and lower

plates, six hex bolts with nuts and washers were used, the bolts being specified in M12 X 75 mm and class 8.8. As the bushings were mounted so that they were supported laterally on the upper and lower bearing plates, the bolts would only exert axial forces.
The coefficient against runoff was verified, according to Eq. (30) (Melconian, 2000):

$$N_y = \frac{S_y}{\sigma_b} \quad \text{.....(30)}$$

The safety coefficient to failure of joint separation was described by Eq. (31) (Melconian, 2000):

$$N_{sep.} = \frac{P_s}{P_{ap.}} \quad \text{..... (31)}$$

To fix the base plate of the central column, six screws were used, being specified in M24 X 100 mm with class of 8.8. The coefficient of flow was verified, using Eq. (30), and the safety coefficient to failure of separation of the joint, using Eq. (31).

RESULTS AND ANALYSIS

According to the calculations carried out in all the stages, it was possible to verify that the crane supported all the efforts. In the case of load applied to the "W" profile, a maximum displacement of -2.12 mm was found, with an inclination angle at the "D" point equal to 0.086 °. For the load applied at point "B", a maximum displacement of -1.09 mm was found, with an inclination angle at point "D", equal to 0,09 °. The normal tension at point "A" was 17.89 MPa, thus presenting a value below the material flow stress. By analyzing the flat bar, a tensile force of 68584 N. The area of the minimum cross section to support the tensile force should be equal to 571.53 mm². To facilitate assembly, a bar with cross-sectional area equal to 967.74 mm² was used, an area larger than that calculated. Through the deformation in the length of the bar, the profile "W" shifted -14.06 mm. The von Mises equivalent stress found by the simulation in the Ansys® software was 80.121 MPa, represented by Fig. 9:

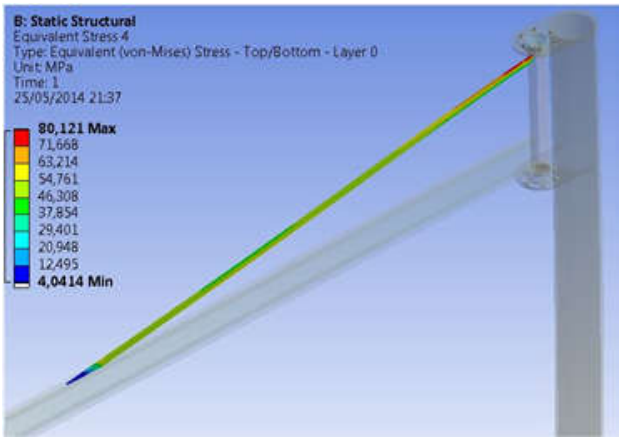

Fig. 9. Analysis of the von Mises voltage on the flat bar

By analyzing the pivot shaft, the minimum diameter for 27.62 mm roller bearing engagement was found. The displacement at the "B" point of the "W" profile caused by the shaft arrow was -1.53 mm. The von Mises equivalent stress, found by the simulation in Ansys® software, was 91,753 MPa, represented by Fig. 10:

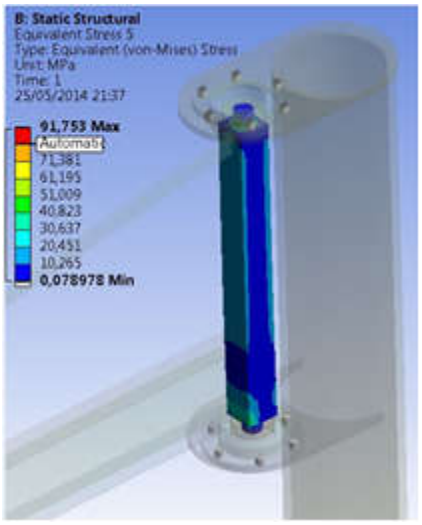

Fig. 10. Analysis of the von Mises voltage of the rotation axis

Analyzing the central column, a displacement of -9.18 mm was found at the "B" point of the "W" profile caused by the displacement of the column. The von Mises equivalent stress, found by the simulation in Ansys® software, was 39.868 MPa, represented by Fig. 11:

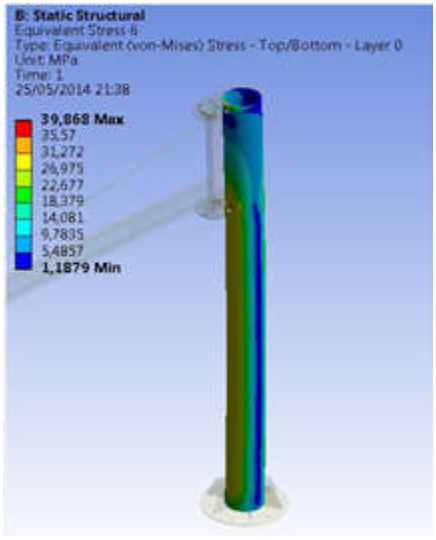

Fig. 11. Analysis of the von Mises voltage of the central column

Taking the sum of the maximum arrow of the components of the structure, a displacement at the "B" point of the "W" profile of -26.89 mm was verified. The displacement performed with Ansys® software analysis was -27.998 mm, according to Fig. 12.

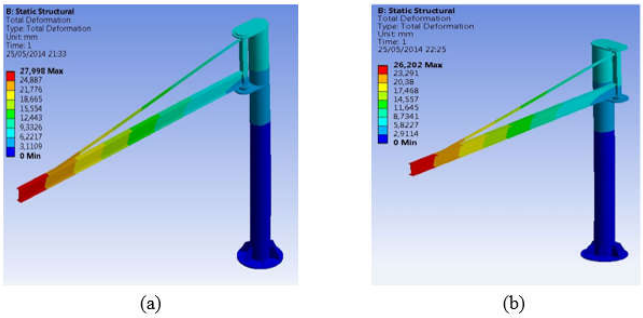

Fig. 12. Analysis of deformation verified by the Ansys® software: a - Position of the boom at 135 °, b - Position of the boom at 45 °

Comparing the calculated results with those obtained with the Ansys® software, one can verify that the values were very close, thus obtaining a proof of the results obtained with the calculations. The highest equivalent voltage found in the crane by the simulation in the Ansys® software was 129.5 MPa, being in the places of union of the shaft with the flat bar and the profile "W", represented by Fig. 13:

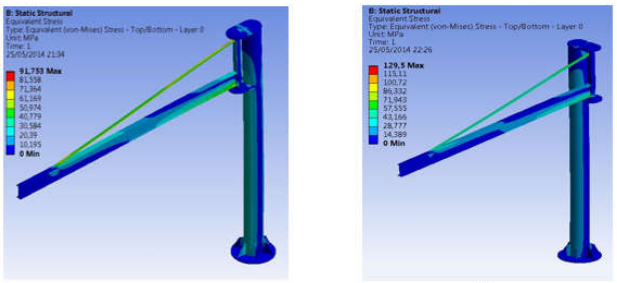

Fig. 13. Analysis of the von Mises tension of the crane: a - Position of the boom at 135 °, b - Position of the boom at 45 °

The bearing selection was obtained through the axial and radial forces, because its internal diameter of 60 mm was already above the minimum diameter required for the shaft with a diameter equal to 27.62 mm. Its stated life is 53217 hours. For the static load coefficient, the result was 4.4, with a value greater than 1.0 guaranteeing the use of the bearing. The coefficient of flow of the screws securing the bushings and the screws securing the base plate of the central column was 1.18 and 1.20, respectively. The safety coefficient to failure of joint separation was 25.1 and 24.57, respectively. The coefficients presented values greater than 1.0 guaranteeing the safety of application. It was possible to verify that with the application of the crane, there was a 34% increase in the manufacture of parts.

Conclusion

With the development of this work, it was possible to arrive at the following conclusions

- The deployment of the rotary crane in the cut and fold sector greatly increases productivity by eliminating the use of the overhead crane for cutting and folding heavy parts;
- The cost of manufacturing and installing the rotary crane is in the range of 70-80% lower than the manufacture and deployment of a crane;
- The results obtained in the Ansys® software were very close to the results obtained with the calculations, proving the results;
- With the maximum working load of 5000N, the displacement of the profile "W" will be imperceptible due to the compensation coefficient adopted.

In relation to future work, it is suggested

- Conduct a study to analyze welded regions;
- Sizing a foundation;
- When implementing the project, carry out an internal procedure by directing the operators to manufacture the heavy parts on the machines that have the crane assistance.

REFERENCES

Açominas. *Catálogo Técnico de Perfis Laminados*, 2003.

Aneziris, O. N., Papazoglouf, I. A., Mud, M. L., Damen, M., Kuiper, J., Baksteen, H., Ale, B. J., Bellamy, L. J., Hale, A. R., Bloemhoff, A., Post, J. G. and Oh, J. 2008. *Towards Risk Assessment for Crane Activities.* Safety Science 46 p.872–884.

Beer, P., Ferdinand, Johnston Jr. and Russell, E. 1995. *Resistência dos Materiais*. 3 ed. São Paulo: Pearson Education do Brasil.

Bucas, S., Rumelhart, P., Gayton, N. and Chateauneuf, A. 2014. *A Global Procedure for the Timedependent Reliability Assessment of Crane Structural Members*. *Engineering Failure Analysis,*

Dubbel and Heinrich, 1974. *Manual do Engenheiro Mecânico.*Vol. 5. 13 ed. São Paulo: Hemus,

Favorit. *Catálogo Técnico de Chapas Laminadas,* 2012.

Fonseca and Eduardo, 2005. *Determinação Indireta das Propriedades Mecânicas de Aço ASTM A36 Laminado com o Uso de Ultra-Som*. UFRGS, Visualizado em 04/04/2014, disponível http://www.lume.ufrgs.b r/bitstream/handle/10 183/6662/000488009.pdf?sequence=1&locale=en

Ghosh, A. and Gurumoorthy, K. 2013. *Failure Investigation of a Taper Roller Bearing: A Case Study. Case Studies in Engineering Failure Analysis,* 1 p.110–114.

Hibbeler, R.C. 2005. *Estática: Mecânica Para Engenharia*. Vol. 1. 10 ed. São Paulo: Pearson Prentice Hall,

Jerman, B. and Kramar, J. 2008. *A Study of the Horizontal Inertial Forces Acting on the Suspended Load of Slewing Cranes*. *International Journal of Mechanical Sciences,* 50 p.490–500.

Kłosiński, J. 2005. *Swing-Free Stop Control of the Slewing Motion of a Mobile Crane. Control Engineering Practice* 13 p.451–460.

Marquez, A. A., Venturino, P. and Otegui, J. L. 2014. *Common Root Causes in Recent Failures of Cranes. Engineering Failure Analysis,* 39 p.55–64.

Melconian and Sarkis, 1949 – *Elementos de Máquinas* / SarkisMelconian. – Edição revisada, atualizada e ampliada. – São Paulo: Érica, 2000.

Neupert, J., Arnolda, E., Schneider, K. and Sawodny, O. 2010. *Tracking and Anti-Sway Control for Boom Cranes. Control Engineering Practice,* 18 p.31–44.

NSK. *Catálogo de Rolamentos*, 1997.

****